

# PREDICTING CH<sub>4</sub> ADSORPTION CAPACITY OF MICROPOROUS CARBON USING N<sub>2</sub> ISOTHERM AND A NEW ANALYTICAL MODEL

Jian Sun,<sup>1</sup> Scott Chen,<sup>2</sup> Massoud Rostam-Abadi<sup>1,2</sup> and Mark J. Rood,<sup>\*1</sup>

<sup>1</sup> Department of Civil and Environmental Engineering, University of Illinois at Urbana-Champaign (UIUC), 205 North Mathews Avenue, Urbana IL 61801, USA

<sup>2</sup> Illinois State Geological Survey (ISGS), 615 East Peabody Drive, Champaign IL 62810, USA

## ABSTRACT

A new analytical pore size distribution (PSD) model was developed to predict CH<sub>4</sub> adsorption (storage) capacity of microporous adsorbent carbon. The model is based on a 3-D adsorption isotherm equation, derived from statistical mechanical principles. Least squares error minimization is used to solve the PSD without any pre-assumed distribution function. In comparison with several well-accepted analytical methods from the literature, this 3-D model offers relatively realistic PSD description for select reference materials, including activated carbon fibers. N<sub>2</sub> and CH<sub>4</sub> adsorption data were correlated using the 3-D model for commercial carbons BPL and AX-21. Predicted CH<sub>4</sub> adsorption isotherms, based on N<sub>2</sub> adsorption at 77 K, were in reasonable agreement with the experimental CH<sub>4</sub> isotherms. Modeling results indicate that not all the pores contribute the same percentage V<sub>m</sub>/V<sub>s</sub> for CH<sub>4</sub> storage due to different adsorbed CH<sub>4</sub> densities. Pores near 8-9 Å shows higher V<sub>m</sub>/V<sub>s</sub> on the equivalent volume basis than does larger pores.

## INTRODUCTION

Activated carbon usually has a heterogeneous pore structure due to the structural complexity and randomness.<sup>1</sup> The distribution of pore sizes is a critical parameter for characterizing the adsorbent, when the adsorption potential is a dominant factor. Adsorption density is strongly dependent on the adsorbent's pore size ( $w$ ). For instance, adsorption is enhanced in micropores ( $w < 20$  Å) due to overlap of the force field created by the opposing pore walls. For applications such as natural gas storage, the adsorbent should be prepared in such a way that it has minimum mesopore ( $20 \text{ Å} < w < 500 \text{ Å}$ ) and macropore ( $w > 500 \text{ Å}$ ) volume and maximum micropore volume. In particular,  $w$  for micropores should be near 8 Å; the optimal pore size for CH<sub>4</sub> adsorption.<sup>2</sup> In this study  $w$  is defined as the distance between the edges of the carbon atoms in opposite pore walls. The pores are modeled as slits consisting of two infinite graphite planes.

A number of PSD models have been developed on the basis of N<sub>2</sub> adsorption at 77 K. Although the models provide great insights, there is apparent lack of consistency in the modeled PSD results<sup>3</sup> due to their different theoretical foundations and assumptions. Well-accepted PSD characterization methods include MP,<sup>4</sup> DRS,<sup>5</sup> JC,<sup>6</sup> HK<sup>7</sup> and, more recently, SNAP<sup>8,9</sup> and DFT.<sup>10</sup> SNAP is one of the latest PSD methods based on numerical results from Mean-Field Density Functional Theory (MFT).<sup>8,9</sup> SNAP uses a pre-assumed log normal distribution function to model N<sub>2</sub> adsorption at 77 K. DFT (Micromeritics) is one of the latest PSD methods based on Non-local MFT.<sup>10</sup> DFT employs a Regularization technique to solve the generalized adsorption isotherm (GAI)<sup>8,11</sup> which results in a discrete PSD. Another version of DFT (Quantachrome) is based on Local MFT, which neglects the adsorbate-adsorbate interactions.

The objective of this study is to model and correlate N<sub>2</sub> and CH<sub>4</sub> adsorption on microporous carbon through an analytical approach. A PSD model is developed on the basis of a 3-D isotherm equation without pre-assumed distribution functions. Prediction of CH<sub>4</sub> adsorption isotherm is carried out by correlating the N<sub>2</sub> and CH<sub>4</sub> adsorption for select adsorbents.

## MODEL DESCRIPTION

Taking an approach similar to Chen and Yang's 2-D adsorption isotherm equation,<sup>12</sup> a 3-D adsorption isotherm equation was developed,<sup>13</sup>

$$\ln \frac{\rho'}{\rho^g} + \frac{8\eta - 9\eta^2 + 3\eta^3}{(1-\eta)^3} + \frac{1}{k_B T} \frac{a}{b} \left( \ln(1+4\eta) - \frac{4\eta}{1+4\eta} \right) + \frac{\Phi}{k_B T} = 0 \quad (1)$$

for a given pore size and geometry (slits), with a mean force field  $\Phi$ . The classical Dubinin-Stoeckli (DS) inverse relationship,<sup>14</sup> is used for its simplicity to evaluate the mean force field as a function of pore size.  $\rho^g$  and  $\rho'$  are volume number densities of the gas and adsorbed phases,

respectively.  $\eta$  is the pore filling fraction. The second term in Eq. 1 describes the short-range repulsive force between adsorbate molecules, while the third term represents the long-range attractive force between adsorbate molecules. The fourth term refers to the interaction between adsorbate and adsorbent. For low adsorption density (close to bulk gas density), the packing fraction is close to zero (so are the second and third terms in Eq. 1), thus the equation reduces to Henry's law. In comparison with the 2-D equation,<sup>12</sup> 3-D adsorption density can be obtained with the 3-D equation. Therefore,  $N_2$  and  $CH_4$  adsorption density and PSD based on  $N_2$  adsorption can be determined.

For  $N_2$  adsorption at 77 K, phase transition from gas to liquid takes place in micropores when adsorption density increases substantially due to pore filling. To include this feature and assure a realistic adsorption density, a modified DR equation is used to calculate adsorption density after pore filling.<sup>15</sup>

$$\rho = \rho_l \exp \left[ - \left( \frac{A}{\beta E_0} \right)^2 \right] \quad (2)$$

where  $\rho$  is the density of adsorbed phase.  $\rho_l$  is the density of saturated liquid  $N_2$ .  $A$  is the differential molar work,  $\beta$  is the affinity coefficient and  $E_0$  is the adsorption characteristic energy. The pore filling fraction  $\theta$  can be expressed as  $\rho/\rho_l$ .

Correlation between pore filling pressure and critical pore size in the 3-D model was obtained from MFT<sup>8,9</sup> to describe the discontinuous jump in the  $N_2$  adsorption isotherm.<sup>13</sup> In other words, the adsorption densities prior to and after pore filling are calculated by the 3-D equation and by the modified DR equation, respectively.

To obtain the PSD, the GAI is formulated as:<sup>8,11</sup>

$$n(P') = \int_0^{\infty} \rho(P', w) f(w) dw \quad (3)$$

$n(P')$  is the amount of adsorbed  $N_2$  at a relative pressure  $P'$  ( $= P/P_0$ ) obtained directly from the experimental adsorption isotherm,  $\rho(P', w)$  is the adsorbate density calculated using the 3-D adsorption isotherm (Eq. 1) and modified DR equation (Eq. 2), and  $f(w)$  is the distribution of pore volume as a function of  $w$ . Eq. 3 is broken down into a set of linear equations solved using least squares error minimization.<sup>13</sup>

## MATERIALS USED

Two activated carbon fiber (ACF) samples (ACF-15 and ACF-25) obtained from American Kynol, Inc. (New York, NY) were used as adsorbents for PSD modeling. ACF-15 has the shorter activation time (lower burn-off and higher yield) compared to ACF-25. Norit Row (American Norit) is used to compare PSD results by DFT and the 3-D model.  $N_2$  adsorption data and DFT results for Norit Row were obtained from Kruk.<sup>16</sup> Other commercial carbons used are BPL (Calgon Carbon), and AX-21 (Amoco). The 77 K  $N_2$  adsorption isotherm of BPL and AX-21 was measured with a Micromeritics ASAP2400 ( $P/P_0$ :  $10^{-3}$  to 1).

## RESULTS AND DISCUSSION

### Optimal Pore Size for $CH_4$ Adsorption

Multiple layer adsorption does not occur at ambient temperature for  $CH_4$  because it is a supercritical gas. Therefore, there must be an optimal pore size associated with the maximum  $CH_4$  adsorption density. Densities of adsorbed  $CH_4$  at 3.4 MPa (500 psia) and 300 K on an ideal adsorbent with various pore sizes are calculated using Eq. 1. The affinity coefficient  $\beta$  for  $CH_4$  is calculated using the following equation

$$\beta = \frac{[P']}{[P']_0} = 0.353 \quad (4)$$

$[P']$  and  $[P']_0$  are the parachors of  $CH_4$  and benzene, respectively, which can be obtained from standard references.<sup>17</sup> Dependence of adsorbed  $CH_4$  density on pore size is plotted in Figure 1. The optimal pore size with a maximum adsorption capacity is  $\approx 8.0$  Å, closely matching the results obtained by computer simulation.<sup>2</sup>

### PSD Characterization of Activated Carbon Fibers

PSDs for ACF-15 and ACF-25 obtained by the 3-D model are presented in Figure 2. The

micropore volume and pore volume for  $w < 100 \text{ \AA}$  from the 3-D model are 0.363 and 0.988  $\text{cm}^3/\text{g}$  respectively (Table 1). Increased pore volume and pore widening are expected for ACF-25 compared to ACF-15. These features are well illustrated in Figure 2. Calculated  $\text{N}_2$  isotherms using the 3-D model and the corresponding experimental isotherms for the two ACF samples are also presented in Figure 2. Good agreement exists in all cases.

Comparisons of PSD results for ACF-25 by MP, JC, HK and the 3-D model are summarized in Figure 3. In contrast to the PSDs by JC and HK, a multiple modal PSD for ACF-25 is revealed by the 3-D model, which corresponds to the inflections in the experimental isotherm. MP method indicates the PSD maximum is about 8  $\text{\AA}$  (Table 1). This is due to the MP method not considering the enhanced adsorption in micropores. The adsorption film thickness (related directly to estimated pore size in the MP method) should be greater in micropores than for non-porous materials at a given relative pressure. MP method tends to underestimate the pore size for micropores. The PSD obtained by JC method predicts a single mode and extends further into the mesopore region (maximum at 16  $\text{\AA}$ ). Such result is presumably caused by use of the DR equation and the initial constraint associated with the pre-assumed normal distribution for the PSD. Compared with the others, HK method gives the smallest PSD maxima for both ACF samples (Table 1). It does not appear to respond well to pore widening brought about by the extent of activation for ACF-25. HK method underestimates the pore size due to the progressive pore filling mechanism.

#### Comparison of PSDs by DFT and 3-D Model

PSD results using the DFT method<sup>10</sup> for Norit Row is provided in Figure 4. The PSD results by DFT are reproduced by normalizing the pore volumes to the corresponding pore size intervals and taking the center point of each size interval as the corresponding pore size. PSD by DFT is usually presented as a discrete bar chart.<sup>18,19</sup> PSD results by the 3-D model based on the same  $\text{N}_2$  isotherm is also plotted in Figure 4. Reasonable agreement can be observed between the two methods, although the PSD maximum by DFT is 0.5  $\text{\AA}$  larger than that by the 3-D model.

#### Prediction of $\text{CH}_4$ Adsorption Isotherm

Prediction of  $\text{CH}_4$  adsorption isotherm at 296 K is carried out with BPL and AX-21 (Figure 5), whose experimental  $\text{CH}_4$  adsorption isotherms were obtained from Sosin.<sup>20</sup> The 3-D equation is used to calculate the  $\text{CH}_4$  adsorption densities (with volume exclusion but no pore filling because  $\text{CH}_4$  is supercritical), which are then combined with the modeled PSDs to obtain  $\text{CH}_4$  adsorption isotherms at 296 K. It is noticed that  $\text{CH}_4$  adsorption is overestimated in the low pressure region and underestimated in the high pressure region by the 3-D model. This is possibly due to the use of the DS inverse relationship to calculate the adsorption potential energy for  $\text{CH}_4$  adsorption. In comparison with experimental results based on a molecular probe study,<sup>21</sup> the DS inverse relationship overestimates the adsorption potential. The potential by the DS relationship also decreases rapidly as the pore size increases,<sup>22</sup> resulting in underestimated adsorbed  $\text{CH}_4$  density. Using the DS relationship for  $\text{N}_2$  adsorption cannot offset this effect, since the modified DR equation is used to calculate the adsorption density after complete pore filling. At high adsorptive pressures, the adsorption density is close to the value of liquid  $\text{N}_2$ , when the DS relationship has negligible contribution to the adsorption density. The prediction may be improved by using other more sophisticated yet more complicated correlation like the HK relationship for carbon and  $\text{CH}_4$ .

Modeling results indicate that not all the pores contribute the same percentage  $\text{Vm}/\text{Vs}$  for gas storage due to different adsorbed  $\text{CH}_4$  densities. Micropores near 8-9  $\text{\AA}$  shows greater volumetric  $\text{CH}_4$  capacity ( $\text{Vm}/\text{Vs}$ ) on the equivalent volume basis than does larger pores. Figures 6 and 7 plot the percentage of pore volume and percentage of  $\text{Vm}/\text{Vs}$  contributed by the pores of ~8, ~9 and ~20  $\text{\AA}$  as functions of activation weight loss for a coal-based carbon series.<sup>23</sup> Around 75% weight loss, volume of ~8  $\text{\AA}$  pores represents only 22% of the total pore volume (percentage pore volume = 22%), but contribute 39% of the total adsorbent's  $\text{Vm}/\text{Vs}$ . The ratio of percentage  $\text{Vm}/\text{Vs}$  to percentage pore volume is 1.8 for ~8  $\text{\AA}$  pores. Similar results can be observed for ~9  $\text{\AA}$  pores. The ratio of %  $\text{Vm}/\text{Vs}$  to % pore volume is 1.6 for ~20  $\text{\AA}$  pores. The ratio is reduced for mesopores and macropores due to the sharp decrease of adsorbed  $\text{CH}_4$  density in these pores.

#### SUMMARY AND CONCLUSIONS

A new analytical PSD model has been developed by solving the GAI for  $\text{N}_2$  adsorption at 77 K using least squares error minimization. Local isotherms for each single pore size is calculated

using a 3-D adsorption isotherm equation, derived from statistical mechanical principles. In comparison to select analytical methods from the literature, this 3-D model offers a relatively realistic PSD description for select reference materials. N<sub>2</sub> and CH<sub>4</sub> adsorption is correlated using the 3-D model for BPL and AX-21. Predicted CH<sub>4</sub> adsorption isotherms are in reasonable agreement with experimental CH<sub>4</sub> isotherms.

**Acknowledgments.** AX-21 was provided by Mega-Carbon Co. N<sub>2</sub> isotherms for ACFs and Norit Row were provided by Drs. Mark Cal and Anthony Lizzio of ISGS and Drs. Michal Kruk and Mietek Jaroniec of Kent State University.

## REFERENCES

1. Gregg, S.J. and Sing, K.S.W. *Adsorption, surface area and porosity* Academic, London, 1984
2. Matranga, K.R.; Stella, A.; Myers, A.L.; Glandt, E. D. *Chem. Eng. Sci.* **1992**, *47*, 1569.
3. Russell, B.P.; LeVan, M.D. *Carbon* **1994**, *32*, 845.
4. Mikhail, R.Sh.; Brunauer, S.; Bodor, E.E. *J. Colloid Interface Sci.* **1968** *26* 45
5. Stoeckli, H.F. *J. Colloid Interface Sci.* **1977**, *59*, 184.
6. Jaroniec, M.; Choma, J. *Mater. Chem. Phys.* **1986**, *15*, 521.
7. Horvath, G.; Kawazoe, K. *J. Chem. Eng. Jpn.* **1983**, *16*, 470.
8. Seaton, N.A.; Walton, J.P.R.B.; Quirke, N. *Carbon* **1989**, *27*, 853.
9. Lastoskie, C.; Gubbins, K.E.; Quirke, N. *J. Phys. Chem.* **1993**, *97*, 4786.
10. Olivier, J.P. *J. Porous Mater.* **1995**, *2*, 9.
11. McEnaney, B. *Carbon* **1988**, *26*, 267.
12. Chen, S.G.; Yang, R.T. *Langmuir* **1994**, *10*, 4244.
13. Sun, J.; Rood, M.J.; Rostam-Abadi, M. in *Extended Abstract the 23<sup>rd</sup> Biennial Conference on Carbon*, State College, PA, 1997, pp. 348
14. Dubinin, M.M. in *Progress in Surface and Membrane Science* Academic 1-70, 1975
15. Sun, J.; Brady, T.A.; Rood, M.J.; Lehmann, C.M.; Rostam-Abadi, M.; Lizzio, A.A. *Energy and Fuel* **1997**, *11*, 316. (b)
16. Kruk, M.; Jaroniec, M. *Adsorption* **1996**, *3*, 209.
17. Quayle, O.R. *Chem. Rev.* **1953**, *53*, 439.
18. Kruk, M.; Jaroniec, M. in *Extended Abstract the 23<sup>rd</sup> Biennial Conference on Carbon*, State College, PA, 1997, pp. 106
19. Olivier, J.P.; Conkin, W.B.; Szombathely, M.V. in *Characterization of Porous Solids III* Elsevier Amsterdam, 1994
20. Sosin, K.A.; Quinn, D.F. *J. Porous Material* **1995**, *1*, 111.
21. McEnaney, B. *Carbon* **1987**, *25*, 457.
22. Chen, S.G.; Yang, R.T. *J. Colloid Interface Sci.* **1996**, *177*, 298.

**Table 1** Summary of PSD information for ACFs-15 and 25 by MP, JC, HK and the 3-D Model

Method	PSD Max. [Å]	ACF-15		PSD Max. [Å]	ACF-25	
		Micropore volume [cm <sup>3</sup> /g]	Pore volume [cm <sup>3</sup> /g]		Micropore volume [cm <sup>3</sup> /g]	Pore volume [cm <sup>3</sup> /g]
MP	5.1	0.318	0.322	7.7	1.066	1.109
JC	9.5	0.343	0.343	15.5	0.504	0.865
HK	5.3*	0.333	0.336	5.8	0.801	0.843
3-D	7.0	0.363	0.363	9.0	0.988	1.070

\* Actual maximum should be less.

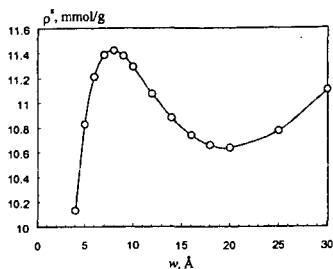


Figure 1 The optimal pore size for CH<sub>4</sub> adsorption.

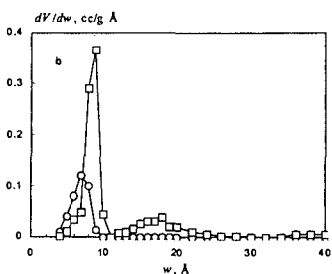
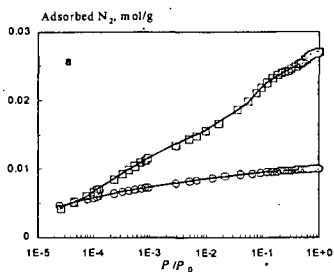


Figure 2 Experimental (symbols) and calculated (lines) N<sub>2</sub> adsorption isotherm at 77 K (a) and PSDs for ACFs-15 (circles) and 25 (squares) by the 3-D model (b).

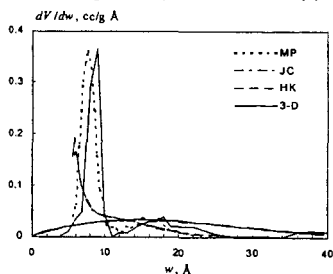


Figure 3 Comparison of PSDs for ACF-25 by MP, JC, HK and the 3-D model.

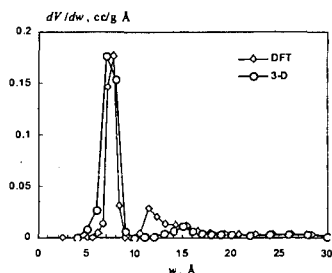


Figure 4 PSD results for Norit Row by DFT and the 3-D model.

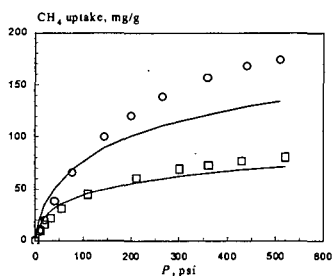


Figure 5 Experimental (symbols) and predicted (lines) CH<sub>4</sub> adsorption isotherms for AX-21 (circles) and BPL (squares).

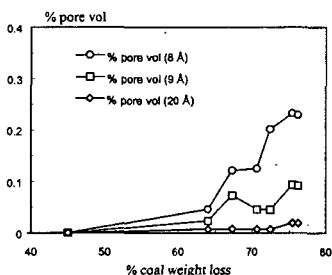


Figure 6 Percentage pore volume vs weight loss in the preparation of a serial coal-based steam-activated carbon at 800°C.

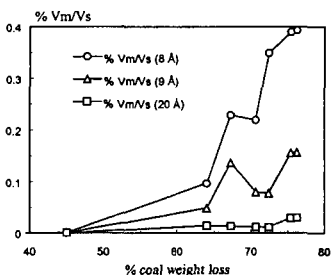


Figure 7 Percentage Vm/Vs vs weight loss.